Protein Engineering, Design & Selection vol. 25 no. 10 pp. 531–537, 2012
Published online August 22, 2012 doi:10.1093/protein/gzs047

Mechanisms of self-association of a human monoclonal antibody CNTO607

Deidra Bethea[†], Sheng-Jiun Wu[†], Jinquan Luo, Linus Hyun, Eilyn R.Lacy, Alexey Teplyakov, Steven A.Jacobs, Karyn T.O'Neil, Gary L.Gilliland and Yiqing Feng[1]

Biologics Research, Biotechnology Center of Excellence, Janssen Research & Development, LLC, 145 King of Prussia Road, Radnor, PA 19087, USA

[1]To whom correspondence should be addressed.
E-mail: yfeng8@its.jnj.com

Received March 19, 2012; revised July 16, 2012; accepted July 18, 2012

Edited by Dennis Burton

Some antibodies have a tendency to self-associate leading to precipitation at relatively low concentrations. CNTO607, a monoclonal antibody, precipitates irreversibly in phosphate-buffered saline at concentrations above 13 mg/ml. Previous mutagenesis work based on the Fab crystal structure pinpointed a three residue fragment in the heavy chain CDR-3, $_{99}$FHW$_{100a}$, as an aggregation epitope that is anchored by two salt bridges. Biophysical characterization of variants reveals that F99 and W100a, but not H100, contribute to the intermolecular interaction. A K210T/K215T mutant designed to disrupt the charge interactions in the aggregation model yielded an antibody that does not precipitate but forms reversible aggregates. An isotype change from IgG1 to IgG4 prevents the antibody from precipitating at low concentration yet the solution viscosity is elevated. To further understand the nature of the antibody self-association, studies on the Fab fragment found high solubility but significant self- and cross-interactions remain. Dynamic light scattering data provides evidence for higher order Fab structure at increased concentrations. Our results provide direct support for the aggregation model that CNTO607 precipitation results primarily from the specific interaction of the Fab arms of neighboring antibodies followed by the development of an extensive network of antibodies inducing large-scale aggregation and precipitation.

Keywords: aggregation/monoclonal antibody/protein engineering/solubility/self-association

Introduction

Monoclonal antibodies (mAbs) comprise a class of therapeutic drugs that has experienced the fastest growth over the last decade, addressing many unmet medical needs. With the increasing number of antibody therapeutics, it has been found that high-concentration formulations for subcutaneous delivery are more convenient and economical than conventional intravenous delivery (Shire, 2009). The most common and challenging issues encountered in developing high concentration protein biopharmaceutical formulations are protein aggregation and high viscosity. The molecular nature of the interactions is often difficult to delineate. Although hydrophobic interactions are considered to be a major contributor, other factors that enhance aggregation have been identified (Shire *et al*., 2004). The self-association of a protein therapeutic can sometimes be circumvented by using proper formulation conditions, but there is no guarantee that these approaches will succeed.

The nature of self-association of antibodies has been the focus of several studies (e.g. (Kanai *et al*., 2008; Nishi *et al*., 2011; Yadav *et al*., 2011). Shire and colleagues investigated the high viscosity of a mAb in a high-concentration formulation (Kanai *et al*., 2008). By systematically studying the intact antibody as well as antibody fragments, they identified Fab–Fab interaction as the primary source of self-association, and showed that multiple binding sites exist on the Fab fragment forming self-association networks that lead to high viscosity. Furthermore, they found by swapping charged residues between two antibodies that exposed charged residues in the CDR of one antibody were critical for the self-association and highly viscous behavior of the antibody at high concentrations (Yadav *et al*., 2011). In another study investigating the self-association of an antibody under low-ionic-strength conditions, Nishi and colleagues found that interactions involving the Fc domains were responsible for the aggregation (Nishi *et al*., 2011). These studies and others are leading to a better understanding of the molecular mechanism responsible for self-association and will help in designing antibodies that are less prone to aggregation (Philo and Arakawa, 2009).

CNTO607 is a potent fully human IgG1 mAb against interleukin (IL)-13. It has poor solubility at neutral pH and precipitates in phosphate-buffered saline (PBS) buffer at concentrations above 13 mg/ml. Various protein engineering strategies based on the 3D structure of the CNTO607 Fab fragment were applied to CNTO607 and some succeeded in improving the solubility while retaining activity (Wu *et al*., 2010). The previous efforts pinpointed the aromatic triad $_{99}$FHW$_{100a}$ in the heavy chain (HC) CDR-3 as the aggregation epitope (Wu *et al*., 2010). Based on the tetrameric interaction of the CNTO607 Fab molecules in the crystal structure, we proposed a CNTO607 aggregation model in which the Fab molecules interact with each other through the aromatic residues at $_{99}$FHW$_{100a}$ and a pair of charge interactions involving D50 and D51 in the light chain (LC) and K210 and K215 in the CH1 domain. These interactions lead to mAb precipitation at high protein concentrations due to the bivalency of the mAb. In the studies reported here, site-directed mutagenesis is combined with biophysical characterization tools to test the CNTO607 aggregation model. The mutagenesis efforts focused on the aggregation epitope and the proposed charge interactions that occur in the aggregation model. The isotype effect of the antibody was also

[†]D. Bethea and S-J. Wu contributed equally to this manuscript.

investigated. Self-interaction chromatography (SIC), cross-interaction chromatography (CIC), dynamic light scattering (DLS) and viscosity measurements were used to characterize the resulting variants. In addition, the CNTO607 Fab was shown to be highly soluble but has significant self-interaction propensity. Our results provide evidence that the self-association of CNTO607 is primarily the result of the proposed Fab–Fab interactions that lead to the formation of large mAb networks.

Materials and methods

Mutagenesis, expression and purification of antibodies

Gene-specific primers were designed and synthesized based on the HC V-region of CNTO607. The primers contained flanking HindIII and EcoR1 restriction enzyme sites for cloning into the Lonza pEE GS (glutamine synthetase) vector which contains human IgG1 constant regions. CNTO607 HC expression plasmid was designated as p3401. The LC V-region of CNTO607 was cloned into the pEE GS vector which contains human lambda constant regions. CNTO607 LC expression plasmid was designated as p3408.

The plasmids, p3401 and p3408, were used as templates to generate different variants either on CNTO607 HC or LC. Listed in Table I are the various mutations that were introduced using a QuikChange site-directed mutagenesis kit (Stratagene, Cat# 200522).

CNTO607 used in these studies was produced from an SP2/0 stable cell line. The mutant antibodies were transiently co-expressed by HC and LC plasmids in either HEK293E or CHO cells. Antibody variants were expressed transiently in 1 l volume HEK293E or CHO transfections. Cell-line specific, HEK293E or CHO, differences in antibody solubility among CNTO607 variants were not observed. For each transfection, individual tubes containing 150 μg each of LC and HC DNA and Lipofectamine 2000 (Invitrogen Cat# 11668027) were diluted with 20 ml OptiMem media. The mixtures were incubated at room temperature for 5 min before combining the contents of both tubes and incubating for an additional 20 min at room temperature. The DNA/Lipofectamine/OptiMem complex was added drop-wise directly into media and the cells were then placed in the incubator for 24 h. The transfection media was replaced with 293SFMII production media (Invitrogen Cat# 11686029) 24 h later. After 6 days the conditioned media were harvested for purification. Antibodies were purified from the harvested media using MabSelect SuRe resin (GE Healthcare, Cat# 17-5438-03). The purity of the antibodies was analyzed by sodium dodecyl sulfate-10% polyacrylamide gel electrophoresis according to Laemmli (1970).

Solubility measurements

The solubility of the antibodies and the Fab fragment were determined as described in (Wu *et al*., 2010). Briefly, experiments were carried out using the ultrafiltration method (Haire and Blow, 2001; van Reis and Zydney, 2001; Moore and Kery, 2009). Antibodies were concentrated using VIVAspin6 concentrator with 10 000 MWCO (vs0602) membrane and centrifuged at speeds of 4000–10 000 r.p.m. at 23°C. Prior to concentration, each sample was dialyzed into PBS buffer. Samples were intermittently inspected visually for any signs of precipitation during the concentration process until the desired concentration was obtained. After concentration, all samples were transferred to clean glass tubes and stored overnight at 4°C. The next day, the concentration of the solution was determined by diluting the sample 50-fold in PBS and measuring the absorbance at 280 nm using a Nanodrop Spectrophotometer.

CIC experiment

Polyclonal human IgG or CNTO607 was coupled to a Hi-Trap *N*-hydroxysuccinimide (NHS) ester 1 ml chromatography column (GE Healthcare, Piscataway, NJ, USA) by adding 3 ml of a 10 mg/ml solution of the antibody in coupling buffer (0.1 M $NaHCO_3$ pH 8.1, 0.5 M NaCl). The detailed chromatographic procedure and the determination of the retention factor k′ for each sample was carried out according to Jacobs *et al*. (2010). All chromatography measurements were performed using a Beckman Coulter System Gold high-performance liquid chromatography (HPLC) or an Ettan-LC HPLC system equipped with an autosampler at room temperature.

SIC

For each SIC experiment, the antibody was coupled to Toyopearl AF-tresyl-650M chromatography resin (Tosoh Biosciences, Montgomeryville, PA, USA) as described in Jacobs *et al*. (2010). Final volume of the column was ∼1 ml. Peaks were visualized by monitoring the absorbance at 215 nm. Retention times were determined using the HPLC Ettan LC system UNICORN software. The chromatographic retention factor k′ was calculated as previously described (Payne *et al*., 2006). The retention time (T_m) of an unretained

Table I. Characterization of CNTO607 and variants

CNTO607 variants	Solubility (mg/ml)	k' by CIC of IgG column	k' by CIC of CNTO607 column	Relative binding affinity[a]	B_{22}^b	pI
IgG1	13	1.01 ± 0.04	1.09 ± 0.07	1	−6.9	7.4
Fab	>160	0.53	n.d.[c]	1.08	−17	7.6
F99A/H100A/W100aA	>164	0.04 ± 0.02	0.03 ± 0.00	No binding	−0.7	7.7
F99A	n.d.	0.05 ± 0.02	0.04	No binding	n.d.	n.d.
H100A	n.d.	n.d.	∼1.0	0.2	n.d.	n.d.
W100aA	>116	0.08 ± 0.02	0. 09 ± 0.03	0.08	−0.2	7.7
K210T/K215T	>100	1.74	n.d.	0.8	n.d.	6.5
IgG4	>110	0.39	0.40 ± 0.00	0.9	−0.73	6.0

[a]Relative binding affinity was determined by K_D of IgG1/K_D of variant. The K_D value for CNTO607 IgG1 is 18.4 pM.
[b]The unit for B_{22} is 10^{-4} (mol ml/g^2).
[c]n.d. Not determined.

sample was determined by measuring the retention time of a mAb and acetone on an uncoupled column of similar volume to the protein-coupled column. The T_m was then calculated by dividing this uncoupled column retention time by the retention time of acetone on the uncoupled column and multiplying by the retention time of acetone on the protein coupled column. B_{22} was determined by using the relationships given below as described earlier by Payne *et al.* (2006).

$$B_{22}=\frac{\mathrm{NA}}{\mathrm{MW}^2}\left(\mathrm{BHS}-\frac{k'}{\mathrm{phi2rho}}\right) \quad (1)$$

where NA is Avogadro's number, MW is the molecular weight of the protein, BHS is the calculated exclusion volume and phi2 and rho are calculated from the properties of the matrix according to a published method (Payne *et al.*, 2006).

Viscosity measurement

The viscosity of protein solutions was measured using an m-VROC viscometer (RheoSense Inc., San Ramon, CA, USA). Samples of varying concentration (0.5–10 mg/ml) were measured at 25°C in either duplicate or triplicate depending on the sample size. After each measurement the system was washed with cleaning agent 1% Aquet, followed by washing with water and subsequently with the buffering system of the sample.

DLS experiment

Particle sizes and distributions of all samples were determined on a DynaPro Plate Reader DLS instrument (Wyatt Technologies Corporation) at 20°C. Measurements were made using a Corning® 384 well black plate with clear flat bottom polystyrene (CLS3540) and 40 µl sample in each well at different protein concentrations. For each sample, duplicate measurement was made, and for every measurement 20 runs were performed. The viscosity value for each sample determined as described above is used in the calculation. The refractive index of 1.333 at 589 nm for PBS buffer at 20°C was used (a standard value embedded in the software by the manufacturer). The method of cumulants was used to analyze the data. When a distribution of size is present, the effective radius is obtained by averaging the intensity-weighed radii. These parameters were used by the program to calculate size distributions and hydrodynamic properties of the protein.

Isoelectric-focusing gel analysis

The pI values of the antibodies were determined using Novex® Pre-Cast Vertical pH 3–10 IEF gels according to the manufacturer's protocol (Invitrogen, CA, USA). Two to five microgram of each protein was loaded on the gel. The pI of each antibody listed is the approximate mid-point of the multiple bands observed on the gel. The banding was due to charge heterogeneity introduced by the variability of the N-linked glycosylation.

Binding affinity determination by Biacore analysis

IL-13 was purchased from R&D System (Minneapolis, MN, USA). Surface plasmon resonance experiments were performed as described in (Wu *et al.*, 2010), with some modification. The CNTO607 Fab was captured on the chip surface using an anti-human Fd antibody.

Results

Multiple approaches to characterize the antibodies

A battery of biophysical methods was used to understand how the antibodies behave in solution. The term solubility is defined here as the maximum protein concentration that can be achieved before precipitation is observed by visual inspection. The extent of the self-interaction between two identical molecules in solution is described by the second virial coefficient (B_{22}), which has contributions from hydrophobic effects, van der Waals interactions, hydration forces and electrostatic interactions (Demoruelle *et al.*, 2002). A positive B_{22} value indicates repulsive interactions between molecules while a negative value represents attractive interactions (Neal *et al.*, 1999). In this report, the B_{22} values were derived using SIC (George and Wilson, 1994; Tessier *et al.*, 2002b; Johnson *et al.*, 2009; Gabrielsen *et al.*, 2010). A related method, CIC differs from SIC in that it measures the interaction between two different molecules. The CIC method used here refers to a newly developed antibody solubility screening method based on the cross-interaction between the antibody of question in liquid phase and polyclonal human antibodies or a related antibody immobilized on the column matrix (Jacobs *et al.*, 2010). Extensive retention on a CIC column, reflected by a large retention factor k′ indicates a tendency for the antibody to aggregate at high concentrations. This method, requiring only a few micrograms of proteins, serves as a reliable means to quickly assess whether an antibody will be soluble at concentrations above 100 mg/ml. DLS is another method for investigating the biophysical properties of a protein. It measures the size distribution of proteins in solution based on the diffusion coefficient of the molecules determined from the intensity fluctuations of scattered light on particles. DLS results are highly sensitive to the presence of aggregates due to a strong dependence of the light-scattering intensity on the hydrodynamic radius (Demeester *et al.*, 2005). Finally, determining the viscosity of protein solutions provides another means to probe intermolecular interaction in solution (Maikokera and Kwaambwa, 2009; Sharma *et al.*, 2011). Repulsion of protein molecules in solution suppresses aggregation resulting in low viscosity, while attractions favor self-association resulting in high viscosity. These different methods complement one another providing a comprehensive picture of proteins in solution.

Solution characterization of CNTO607

CNTO607 was characterized in PBS buffer at pH 7.2 using the above methods. As reported by Wu *et al.* (2010), CNTO607 can be concentrated to ~13 mg/ml before irreversible precipitation occurs (Table I). The B_{22} value for CNTO607 was determined to be −6.9. In the SIC and CIC experiments the sample eluted as a broad peak (data not shown), indicating a degree of self-interaction (Neal *et al.*, 1998; Ruppert *et al.*, 2001; Tessier *et al.*, 2002a). The behavior of CNTO607 prior to precipitation was investigated by DLS and viscosity measurements. The hydrodynamic radius of CNTO607 increased progressively from 4.2 nm at

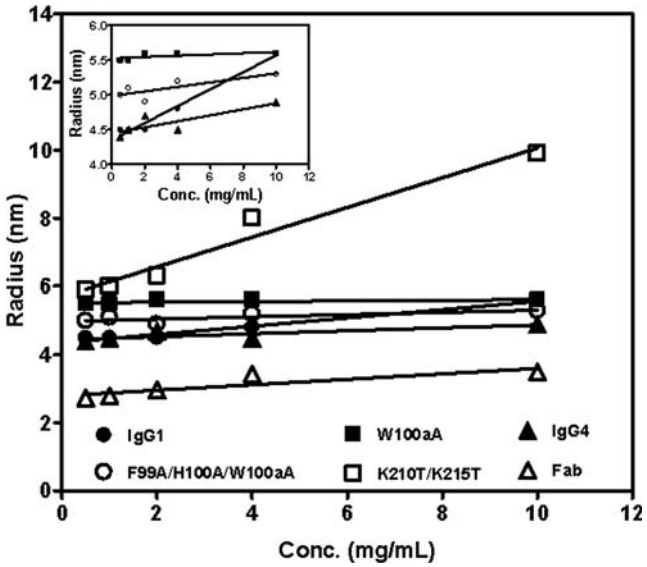

Fig. 1. Hydrodynamic radii of CNTO607 and variants at a series of protein concentrations determined by DLS analysis. The inset is an enlargement of the data for CNTO607, F99A/H100A/W100aA, W100aA and the IgG4 antibody.

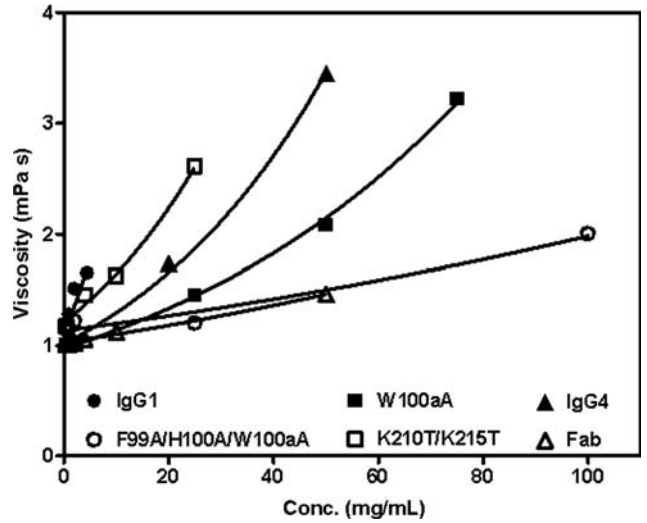

Fig. 2. Viscosity of the CNTO607 and variants solutions at a series of protein concentrations.

0.5 mg/ml to 6.0 nm at 10 mg/ml, suggesting the formation of soluble aggregates at higher concentrations (Fig. 1). In addition, the viscosity of the CNTO607 solution increased sharply upon concentration, making measurement above 4.5 mg/ml very difficult (Fig. 2). Taken together, these results indicate that CNTO607 has a strong tendency to self-associate at moderate concentrations prior to precipitation.

CNTO607 mutants designed to disrupt the Fab–Fab interactions

The high-resolution crystal structure of CNTO607 Fab was solved by Teplyakov *et al.* (2009). In the crystal structure, the CNTO607 Fab forms a nearly symmetrical tetramer, burying the cluster of aromatic residues $_{99}$FHW$_{100a}$ in one of the crystal packing interfaces. The Fab–Fab association is anchored by a pair of salt bridges: LC D50 and D51 of one

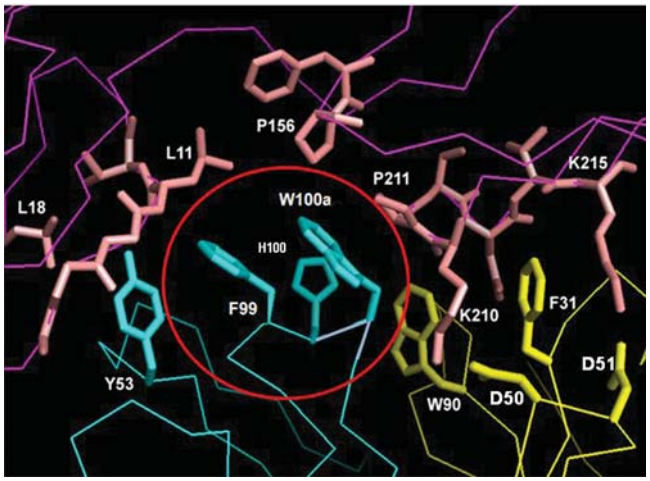

Fig. 3. The crystal structure of CNTO607 Fab showing the intermolecular interaction near the aromatic residue triad. The HC of one Fab is colored cyan and the LC of the same Fab is colored yellow. The adjacent Fab interacting with the first Fab is colored in pink.

Fab molecule interact with HC K210 and K215 of a neighboring Fab molecule (Fig. 3). The interface covers a relatively large surface area of about 500 Å^2 in each Fab structure. It was hypothesized that because of the bivalency of the mAbs, the interactions among the Fab arms lead to large clusters of mAbs at high antibody concentrations (Wu *et al.*, 2010). Indeed, a triple alanine mutant of CNTO607 (F99A/H100A/W100aA) became very soluble, revealing the tripeptide as an aggregation epitope in CNTO607 (Wu *et al.*, 2010).

Additional mutants were generated to further test the CNTO607 aggregation model (Table I). Single mutations F99A, H100A and W100aA were designed to further define the aggregation epitope and its relationship to antigen binding. A double mutant K210T/K215T was also designed to test the strength of the proposed charge interactions involving D50/D51 on the LC and K210/K215 on the HC which anchor the Fab–Fab interface (Fig. 3). Finally, an isotype change from IgG1 to IgG4 was made to probe the effect of changes outside the immediate sphere of the aggregation epitope. The residues involved in the salt bridges, K210T/K215T and D50/D51, are still present upon the isotype change.

Characterization of the CNTO607 mutants

The mutants were produced and assessed for intermolecular interaction by CIC (Jacobs *et al.*, 2010) and activity by IL-13 binding (Table I). The single mutants F99A and W100aA both showed greatly reduced cross-interaction by CIC, the IgG4 antibody showed moderately reduced cross-interaction, while the H100A and K210T/K215T mutants exhibited profiles unchanged or worse than CNTO607 (Fig. 4). The long tails in the CIC profiles of the IgG4 antibody and the K210T/K215T mutant also suggest complex or multi-dimensional interactions. All the single point mutants, similar to the triple mutant F99A/H100A/W100aA, have significantly reduced IL-13 binding affinity. As expected, both the K210T/K215T mutant and the IgG4 antibody maintain affinity to IL-13 similar to that of CNTO607 due to the lack of change in the variable region. Based on the CIC results, W100aA and K210T/K215T mutants and the IgG4 molecule

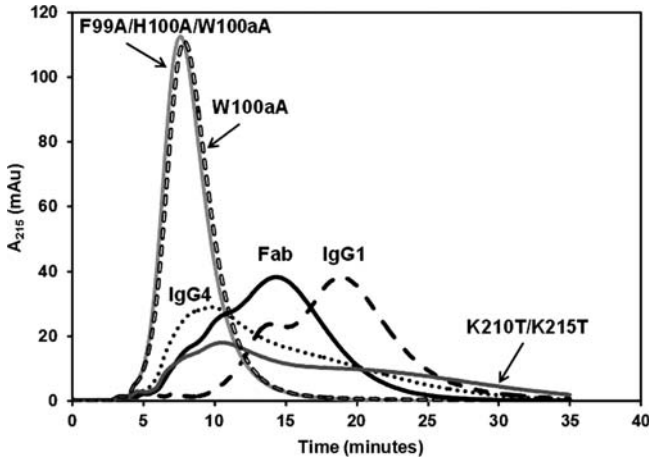

Fig. 4. CIC profiles of CNTO607 and variants.

were selected for scale up and solubility determinations confirmed that they are indeed soluble at >100 mg/ml (Table I). The B_{22} values of the W100aA mutant, the F99A/H100A/W100aA mutant and the IgG4 molecule were found to be > -1.0, confirming significantly diminished self-interaction and increased solubility compared with CNTO607.

Mutants W100aA, K210T/K215T and the IgG4 antibody, together with the previously reported mutant F99A/H100A/W100aA, were further characterized by DLS and viscosity measurement at various protein concentrations. The F99A/H100A/W100aA mutant, the W100aA mutant and the IgG4 antibody exhibited hydrodynamic radii in the expected monomeric antibody range by DLS that were virtually unchanged between 0.5 and 10 mg/ml. The K210T/K215T mutant, however, exhibited a progressively increasing hydrodynamic radius that was significantly larger than expected at higher concentrations (Fig. 1), indicating oligomer formation. The viscosity measurement of these antibody solutions showed that at a given concentration the viscosity follows the order of CNTO607, K210T/K215T, CNTO607 IgG4, W100aA and F99A/H100A/W100aA, with CNTO607 being the most viscous (Fig. 2).

The charge of an antibody can have a profound impact on its self-association interaction (Tanford, 1961). While most of the mutations resulted in only small changes in the pI (Table I and Supplementary Fig. S1), more pronounced differences in pI were observed for the IgG4 antibody and the K210T/K215T variant. IEF gel electrophoresis analysis indicated a ~1.4 point difference between CNTO607 and its IgG4 counterpart, with the IgG4 counterpart being more acidic. After the elimination of two positive charges from its sequence, the K210T/K215T mutant showed a ~1 point decrease in pI relative to CNTO607.

Solution characterization of CNTO607 Fab

The Fab fragment of CNTO607 was studied in order to assess if its self-association is primarily responsible for CNTO607 aggregation. In contrast to the mAb, the Fab fragment of CNTO607 was found to be highly soluble in PBS buffer, reaching a concentration of 160 mg/ml without any visible aggregation. The upper limit of the solubility could not be determined due to a sample quantity limitation. The CIC retention factor of CNTO607 Fab fragment was improved over that of CNTO607, although a significant amount of cross-interaction with the polyclonal IgG still remains. Consistent with the CIC data, the B_{22} of CNTO607 Fab determined by SIC is highly negative (−17) (Table I), indicating strong self-interaction among the Fab molecules. Furthermore, the hydrodynamic radius of CNTO607 Fab showed a progressive increase from 2.7 nm at 0.5 mg/ml to 4.7 nm at 10 mg/ml.

Discussion

We proposed a CNTO607 aggregation model in which the interactions observed in the CNTO607 Fab crystal structure lead to CNTO607 precipitation at high protein concentrations due to the bivalency of the mAb (Wu *et al*., 2010). In the current report, we tested this model by mutagenesis and multiple biophysical characterization methods to identify the important residues involved in the aggregation. We have shown that the data support the above model as the major contributor to the aggregation of CNTO607.

By testing the single point mutants F99A, H100A and W100aA using CIC, SIC and determining their solubilities, we demonstrated that removing the large aromatic side chains of either F99 or W100a disrupts the intermolecular interaction in CNTO607 while eliminating the H100 side chain results in a minimal change to the intermolecular interaction. At the same time, all three single point mutations led to greatly reduced binding affinity to IL-13. In addition to the solubility, the CIC and the SIC measurements, the DLS and viscosity data shed more light on the intermolecular interactions of these antibodies. At 0.5 mg/ml, all the antibodies exhibited hydrodynamic radii in the range of 4–6 nm, within the range reported for monomeric antibody in solution (Liu *et al*., 2010; Driskell *et al*., 2011; Hawe *et al*., 2011; Huo *et al*., 2011). The concentration dependence of the hydrodynamic radii, however, revealed that these antibodies behave somewhat differently. CNTO607 exhibited a smaller than average hydrodynamic radius of slightly above 4 nm at 0.5 mg/ml, which steadily increases to 6 nm at 10 mg/ml, suggesting the formation of aggregates. In contrast, the hydrodynamic radii of the F99A/H100A/W100aA and the W100aA mutants exhibited average antibody hydrodynamic radii of 5–6 nm at the low concentrations, and remained essentially unchanged at higher concentrations. Viscosity measurements provide an independent means to assess self-association when there is no visible precipitation or a large increase in the hydrodynamic radii (Liu *et al*., 2005; Kanai *et al*., 2008). The higher viscosity for mutant W100aA compared with mutant F99A/H100A/W100aA underscores the role of F99 and H100 in the self-association of CNTO607.

The DLS data of the IgG4 antibody show nearly identical hydrodynamic radii at all concentrations measured, similar to the F99A/H100A/W100aA and W100aA mutants. The viscosity of the IgG4 antibody at high concentrations, however, is much higher than that of F99A/H100A/W100aA and W100aA mutants. This indicates that although the isotype change enabled the IgG4 molecule to remain in solution at much higher concentrations than its IgG1 counterpart, a significant number of, and potentially multi-dimensional intermolecular interactions may exist in the IgG4 antibody presumably involving the aggregation epitope. This is in

agreement with the CIC data, where the IgG4 antibody showed a reduced, but still substantial, amount of cross-interaction with either human polyclonal IgG or CNTO607. In contrast to CNTO607 which undergoes irreversible self-association at a relatively low concentration, the self-interaction in the IgG4 variant is reversible in nature manifested by a change in viscosity (Kanai *et al*., 2008).

Based on the amino acid sequences, there is no difference between the IgG1 and IgG4 antibodies in the immediate vicinity of the interaction interface shown in Fig. 3. It is noted that the pI of the IgG4 molecule undergoes a significant change from ~7.4 to 6. It is plausible that at neutral pH the charge repulsion force competes with the intermolecular interactions involving the aggregation epitope in the IgG4 molecule, enabling the antibody to undergo reversible self-association at higher concentrations. The change in solubility resulting from the isotype change implies that the self-association interaction in CNTO607 is relatively weak and can be readily compensated by small changes in the molecule. Indeed, we were unable to detect any significant binding affinity between the CNTO607 molecules using conventional methods such as Biacore. A recent publication reported a significant isotype impact on the solubility of an anti-LINGO-1 antibody (Pepinsky *et al*., 2010). The pI's of those antibodies were at least one unit above neutral pH regardless of the isotype and were thus ruled out as a contributing factor. Whether the pI change prevents our IgG4 antibody from precipitation at neutral pH is the subject of a future investigation.

The behavior of the K210T/K215T mutant was unexpected. This mutant was designed to eliminate the charge interactions with D50 and D51 on the LC of a neighboring mAb which anchor the aromatic triad into the interface. This mutant antibody was found to be much more soluble than CNTO607. The long retention time on the human polyclonal IgG CIC column is not surprising because the aggregation epitope in H-CDR3 and the D50/D51 residues in this mutant antibody can still interact with the CH1 domains present on the immobilized antibodies. Upon further investigation using the DLS and viscosity methods, this antibody was found to aggregate in solution at relatively low concentrations. Although the mechanism of aggregation remains elusive, the constant regions of IgG molecules inherently possess several aggregation hot spots (Chennamsetty *et al*., 2009) so it is possible that while the mutations disrupted the original Fab–Fab interaction it enabled new intermolecular interactions due to the elimination of two positive charges in the CH1domain. This may explain the additional retention of this variant on the CIC column compared with CNTO607. The new interactions do not appear to exacerbate via bivalency, thus no precipitation of the mutant was observed. This finding points to the importance of using multiple experimental methods for antibody characterization, and highlights the challenge for mechanistic studies of protein aggregation. While there is a dominant interaction, multiple weaker interactions may contribute as well.

Our aggregation model predicts that CNTO607 Fab should self-associate but not precipitate. Evidence that self-association occurs within the Fab fragment of CNTO607 comes from the SIC experiment where the B_{22} value for the Fab is excessively negative. The reduced yet still significant retention of the Fab in the CIC experiment is consistent with the aggregation epitope in H-CDR3 interacting in a monomeric manner with the CH1 domains of the polyclonal IgG immobilized on the column matrix. The Fab oligomerization is further supported by the DLS data, where the hydrodynamic radius of the Fab increased from 2.7 nm at 0.5 mg/ml to 4.7 nm at 10 mg/ml. As the concentration increases, the equilibrium appears to shift to higher order oligomer(s). These observations are in agreement with the tetrameric state of the Fab in the crystal, where the protein is highly concentrated. The aggregation model depicted in Fig. 5 illustrates how the Fab–Fab interactions progress to irreversible precipitation of the bivalent antibody. At a concentration of >13 mg/ml when CNTO607 precipitates, the molar equivalent Fab concentration is 8–9 mg/ml when a significant amount of Fab oligomer is present based on the DLS data. According to our model, the antibody networks can begin to form as soon as the Fab arm interactions are abundant and will quickly proceed to an irreversible precipitation.

Our results identified F99 and W100a as two important residues contributing significantly to the intermolecular interactions and support the residue-specific mechanism hypothesis that the Fab interactions serve as the driver for CNTO607 precipitation. Aromatic residues such as tryptophan and phenylalanine on protein surfaces are known to have the potential to

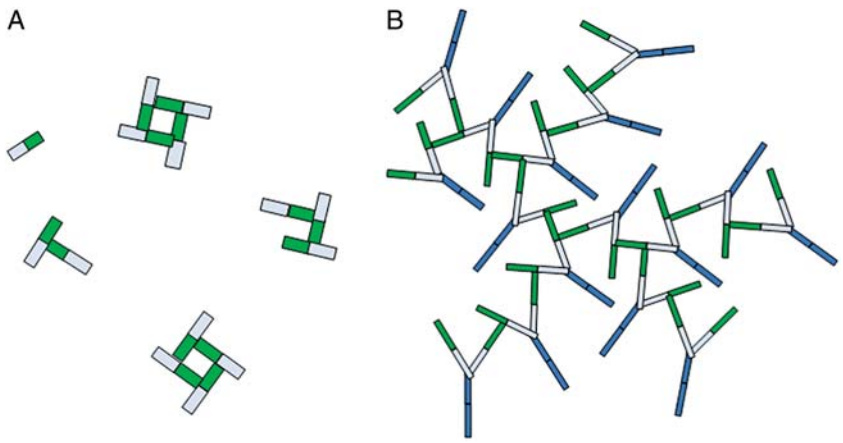

Fig. 5. Cartoon representation of the proposed aggregation model (**A**) CNTO607 Fab; there is one binding site per Fab in the isolated Fab fragments so they can form dimers, trimers and tetramers depending on the protein concentration; (**B**) CNTO607 mAb at high concentrations in solution; each Fab arm of the antibody once involved in oligomerization can form a large cluster of antibodies.

cause low solubility. In a systematic study where solubility of mutants at a single position was compared in RNase Sa, tryptophan and phenylalanine were observed to result in the lowest solubility (Trevino *et al*., 2007). The substitution of any of the three aromatic residues to alanine in the H-CDR3 of CNTO607 was also found to greatly reduce antigen binding affinity. This is not surprising in light of the crystal structure of the IL-13:CNTO607 Fab complex (Teplyakov *et al*., 2009). The aromatic side chains of F99 and W100a not only interact with IL-13 directly but also support each other's orientation enabling the interaction with IL-13. H100, on the other hand, plays a structural role in maintaining the appropriate conformation. Thus, the absence of any of these three side chains led to a reduction in affinity.

In the case of CNTO607 the antigen-binding epitope completely overlaps with the aggregation epitope, making it difficult to engineer high solubility by mutagenesis while maintaining binding affinity. Our results highlight the inherit difficulty to distinguish and differentiate desirable protein–protein interaction from undesirable protein–protein interaction, given that the underlying principles are the same. This may be a more common challenge than previously realized, as suggested by Wang and coworkers who recently reported that aggregation-prone regions occur frequently within the CDR sequences based upon a computational analysis of 29 publicly available high-resolution crystal structures of Fab-antigen complexes (Wang *et al*., 2010). While one may take precaution to avoid the aggregation-prone regions in future library designs, we have found that screening for high solubility early followed by orthogonal characterization method(s) is crucial for the success of therapeutic antibody discoveries. For the engineering approach, our findings suggest that identifying the aggregation epitope in the sequence early is the key to developing effective protein engineering strategies for deriving highly potent and highly soluble antibodies.

Supplementary data

Supplementary data are available at *PEDS* online.

Acknowledgments

We thank James Kang, Ken R.Dixon, Steve Pick, Mark Cunningham, Wei Gao, Steve LaBrenz, Ray Sweet and Rob Hayes for their support, helpful discussions and assistance with this work.

References

Chennamsetty,N., Helk,B., Voynov,V., Kayser,V. and Trout,B.L. (2009) *J. Mol. Biol.*, **391**, 404–413.

Demeester,J., De SSmedt,S.S., Sanders,N. and Haustraete,J. (2005) In Jiskoot,W. and Crommelin,D.J.A. (eds), *Methods for Structural Analysis of Protein Pharmaceuticals: Light Scattering*. AAPS, Arlington, pp. 245–276.

Demoruelle,K., Guo,B., Kao,S., McDonald,H.M., Nikic,D.B., Holman,S.C. and Wilson,W.W. (2002) *Acta Crystallogr. D Biol. Crystallogr.*, **58**, 1544–1548.

Driskell,J.D., Jones,C.A., Tompkins,S.M. and Tripp,R.A. (2011) *Analyst*, **136**, 3083–3090.

Gabrielsen,M., Nagy,L.A., DeLucas,L.J. and Cogdell,R.J. (2010) *Acta Crystallogr. D Biol. Crystallogr.*, **66**, 44–50.

George,A. and Wilson,W.W. (1994) *Acta Crystallogr. D Biol. Crystallogr.*, **50**, 361–365.

Haire,L.F. and Blow,D.B. (2001) *J. Crystal Growth*, **232**, 17–20.

Hawe,A., Hulse,W.L., Jiskoot,W. and Forbes,R.T. (2011) *Pharm. Res.*, **28**, 2302–2310.

Huo,Q., Colon,J., Cordero,A., Jelena Bogdanovic,J., Baker,C.H., Goodison,S. and Pensky,M.Y. (2011) *J. Nanobiotechnology*, **9**, 20–31.

Jacobs,S.A., Wu,S.J., Feng,Y., Bethea,D. and O'Neil,K.T. (2010) *Pharm. Res.*, **27**, 65–71.

Johnson,D.H., Parupudi,A., Wilson,W.W. and DeLucas,L.J. (2009) *Pharm. Res.*, **26**, 296–305.

Kanai,S., Liu,J., Patapoff,T.W. and Shire,S.J. (2008) *J. Pharm. Sci.*, **97**, 4219–4227.

Laemmli,U.K. (1970) *Nature*, **227**, 680–685.

Liu,H.F., Ma,J., Winter,C. and Bayer,R. (2010) *MAbs*, **2**, 480–499.

Liu,J., Nguyen,M.D., Andya,J.D. and Shire,S.J. (2005) *J. Pharm. Sci.*, **94**, 1928–1940.

Maikokera,R. and Kwaambwa,H.M. 2009. Use of Viscosity to Probe the Interaction of Anionic Surfactants with a Coagulant Protein from Moringa oleifera Seeds, *Research Letters in Physical Chemistry*, doi:10.1155/2009/927329 .

Moore,P.A. and Kery,V. (2009) *Methods Mol. Biol.*, **498**, 309–314.

Neal,B.L., Asthagiri,D. and Lenhoff,A.M. (1998) *Biophys. J.*, **75**, 2469–2477.

Neal,B.L., Asthagiri,D., Velev,O.D., Lenhoff,A.M. and Kaler,E.W. (1999) *J. Crystal Growth*, **196**, 377–387.

Nishi,H., Miyajima,M., Wakiyama,N., Kubota,K., Hasegawa,J., Uchiyama,S. and Fukui,K. (2011) *J. Biosci. Bioeng.*, **112**, 326–332.

Payne,R.W., Nayar,R., Tarantino,R., *et al*. (2006) *Biopolymers*, **84**, 527–533.

Pepinsky,R.B., Silvian,L., Berkowitz,S.A., *et al*. (2010) *Protein Sci.*, **19**, 954–966.

Philo,J.S. and Arakawa,T. (2009) *Curr. Pharm. Biotechnol.*, **10**, 348–351.

Ruppert,S., Sandler,S.I. and Lenhoff,A.M. (2001) *Biotechnol. Prog.*, **17**, 182–187.

Sharma,V., Jaishankar,A., Wang,Y.-C. and McKinley,G.H. (2011) *Soft Matter*, **7**, 5950–5960.

Shire,S.J. (2009) *Curr. Opin. Biotechnol.*, **20**, 708–714.

Shire,S.J., Shahrokh,Z. and Liu,J. (2004) *J. Pharm. Sci.*, **93**, 1390–1402.

Tanford,C. (ed) (1961) *Physical Chemistry of Macromolecules*. John Wiley, New York.

Teplyakov,A., Obmolova,G., Wu,S.J., Luo,J., Kang,J., O'Neil,K. and Gilliland,G.L. (2009) *J. Mol. Biol.*, **389**, 115–123.

Tessier,P.M., Lenhoff,A.M. and Sandler,S.I. (2002a) *Biophys. J.*, **82**, 1620–1631.

Tessier,P.M., Vandrey,S.D., Berger,B.W., Pazhianur,R., Sandler,S.I. and Lenhoff,A.M. (2002b) *Acta Crystallogr. D Biol. Crystallogr.*, **58**, 1531–1535.

Trevino,S.R., Scholtz,J.M. and Pace,C.N. (2007) *J. Mol. Biol.*, **366**, 449–460.

van Reis,R. and Zydney,A. (2001) *Curr. Opin. Biotechnol.*, **12**, 208–211.

Wang,X., Singh,S.K. and Kumar,S. (2010) *Pharm. Res.*, **27**, 1512–1529.

Wu,S.J., Luo,J., O'Neil,K.T., *et al*. (2010) *Protein Eng. Des. Sel.*, **23**, 643–651.

Yadav,S., Sreedhara,A., Kanai,S., Liu,J., Lien,S., Lowman,H., Kalonia,D.S. and Shire,S.J. (2011) *Pharm. Res.*, **28**, 1750–1764.